

CASL Joint Industry Council / Science
Council Meeting

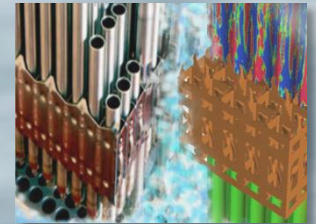
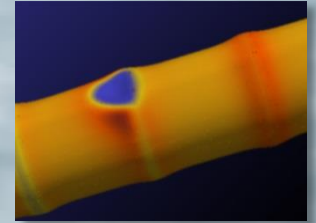
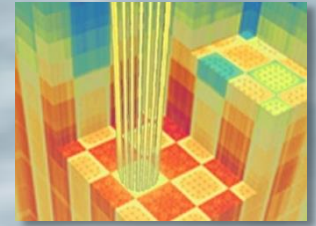
CFD-Based DNB Analysis Methods

Emilio Baglietto, MIT
Dave Pointer, ORNL

October 11-12, 2016



The Consortium for Advanced
Simulation of LWRs
A DOE Energy Innovation Hub



U.S. DEPARTMENT OF
ENERGY

What is challenging about DNB?

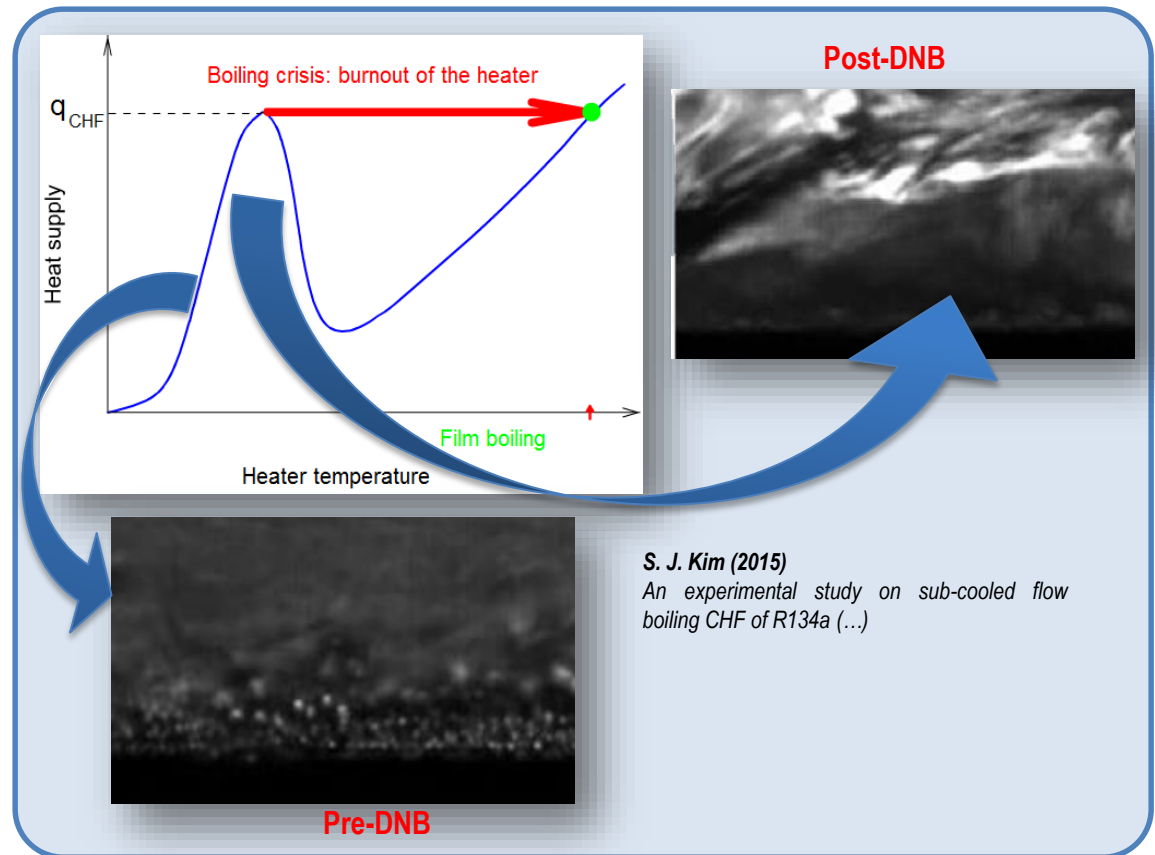
... why using CFD

...what comes to mind?

- Violent transition
- Complex physics
- Lack of understanding
- Decades of research
- **“Moonshot” (Yadigaroglu, 2014)**

...what is the opportunity?

- New generation of experiments
- Mature computational “framework” for CFD



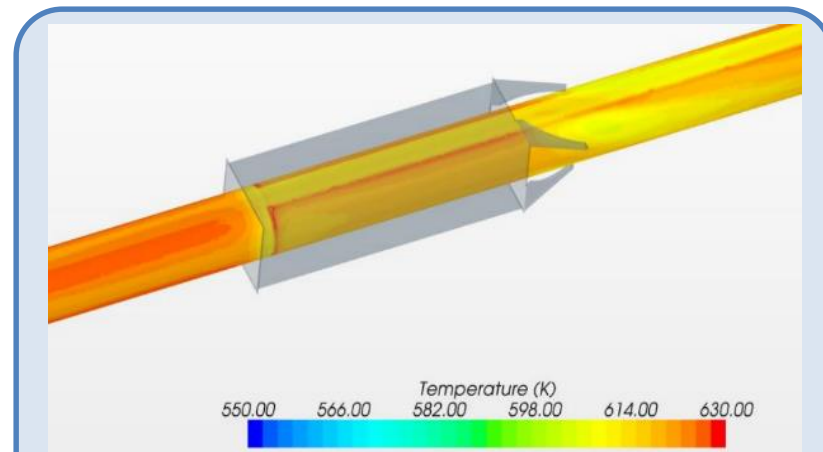
What is challenging about DNB?

... why using CFD

Numerical Correlations	Mechanistic Models	Look-Up Tables
Simply correlate data to a mathematical formula	Attempts to model the physics of the phenomena	Tabulate results for all the operating conditions
<ul style="list-style-type: none"> • Westinghouse W-3 Correlation • Biasi Correlation • Bowring Correlation 	<ul style="list-style-type: none"> • Vapor Column <i>Zuber 1959</i> • Near Wall Bubble Crowding <i>Weisman & Pei 1983</i> • Liquid Sublayer Dryout <i>Katto 1994</i> 	<ul style="list-style-type: none"> • Groeneveld CHF Look-Up Table <i>2006, 1995, 1986</i> • Kirillov CHF Look-Up Table <i>1991</i>
<ul style="list-style-type: none"> • Subchannel codes <i>FLICA4, THINC, COBRA-TF</i> 	<ul style="list-style-type: none"> • Subchannel codes <i>COBRA-IIIC, COBRA-IV-I, MATRA</i> 	<ul style="list-style-type: none"> • System Codes <i>RELAP5, TRACE, CATHARE</i>

Existing models

- Developed a posteriori from experiments
- *Some models do not try to model the physics at all*
- **Use of simple geometries (tubes, channels, annulus...)**
- **Lack predictive power outside validated range**
- **No local surface effect (macro hydrodynamics)**



Proof-of-Concept of DeCART/STAR-CCM+/MAMBA Coupled Simulation (...).
CASL report, 2012

Need for CFD approaches:

- Capture 3D effects (complex geometries)
- Incorporate first principle mechanisms for real predictions

Status of DNB Capabilities in CFD – FY16

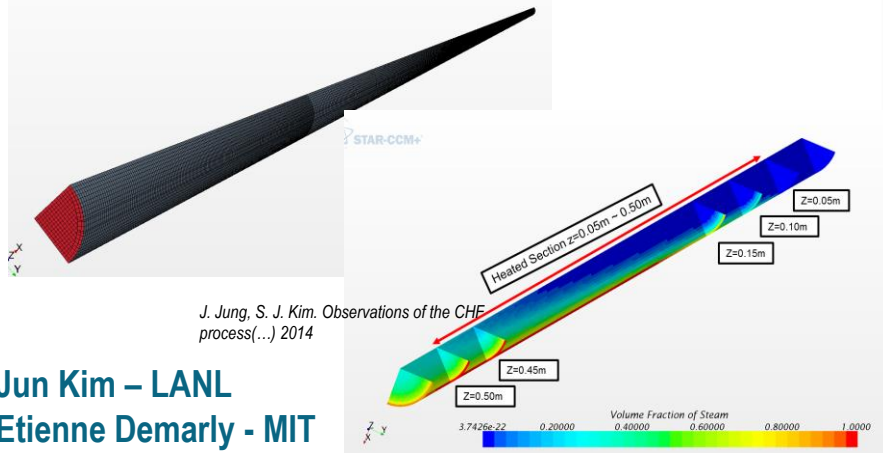
FY16 Completed Milestones (DNB)

#1483	L2:THM.P13.02	Baglietto	PoR-13
Demonstrate DNB analysis methods using CFD (FY16.CASL.009)			
#1489	L3:THM.CFD.P13.04	Seung Jun Kim	PoR-13
LANL - DNB Assessment			
#1498	L3:THM.CLS.P13.09	Buongiorno	PoR-13
Experimental study of subcooled flow boiling heat transfer up to the DNB limit for both uncoated and synthetically CRUD-ed surfaces			
#1503	L3:THM.CLS.P13.01	Balu Nadiga	PoR-13
Hydrodynamic closure evaluation in multiphase flow using STAR-CCM+ and NEPTUNE			
#1493	L3:THM.CLS.P13.03	Junsoo Yoo	PoR-13
Boiling Validation against TAMU Data			
#1492	L3:THM.CLS.P13.05	Baglietto	PoR-13
Robust hydrodynamic closures advancements for PWR application.			
#1497	L3:THM.CLS.P13.08	Hassan	PoR-13
Device-Scale Multiphase Flow Experiments and Data Analysis			
#1500	L3:THM.CFD.P13.01	Podowski	PoR-13
Analyze Mechanistic Models of Subcooled Boiling and CHF in LWR Fuel Assemblies with Spacers			
#1495	L3:THM.CLS.P13.02	Luo	PoR-13
Advanced Boiling Algorithms [Test bed openFOAM]			

GEN-I and GEN-II DNB methods in CFD

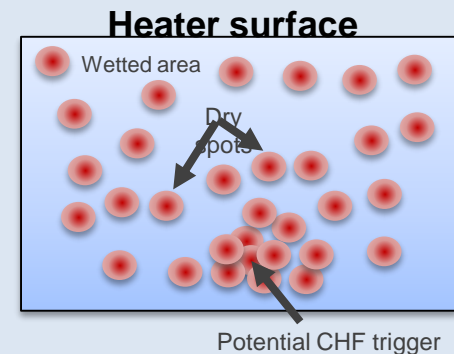
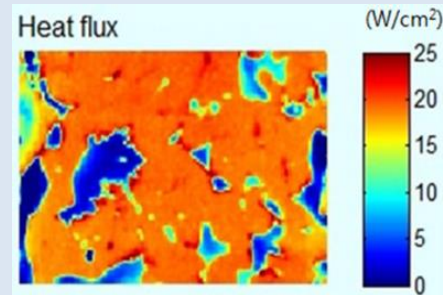
multi-step and multi-approach

- Based on validated GEN-I Hydrodynamic closures
- Macrolayer DNB Method implemented in STAR-CCM+ (a la Weismann-Pei)
- Single Pipe flow DNB test performed at LANL confirm feasibility of the approach
- Currently working on 5x5 performance evaluation



Jun Kim – LANL
Etienne Demarly - MIT

- GEN-II Partitioning Completion
 - Extensive completion / validation activities
- GEN-II Hydrodynamic Closure
 - Lift for higher void fraction / robustness
 - Turbulence and wall treatment for improved predictions
- Novel DNB resolution approach
 - Key to generality
 - Includes surface effects
 - Tight schedule for assessment

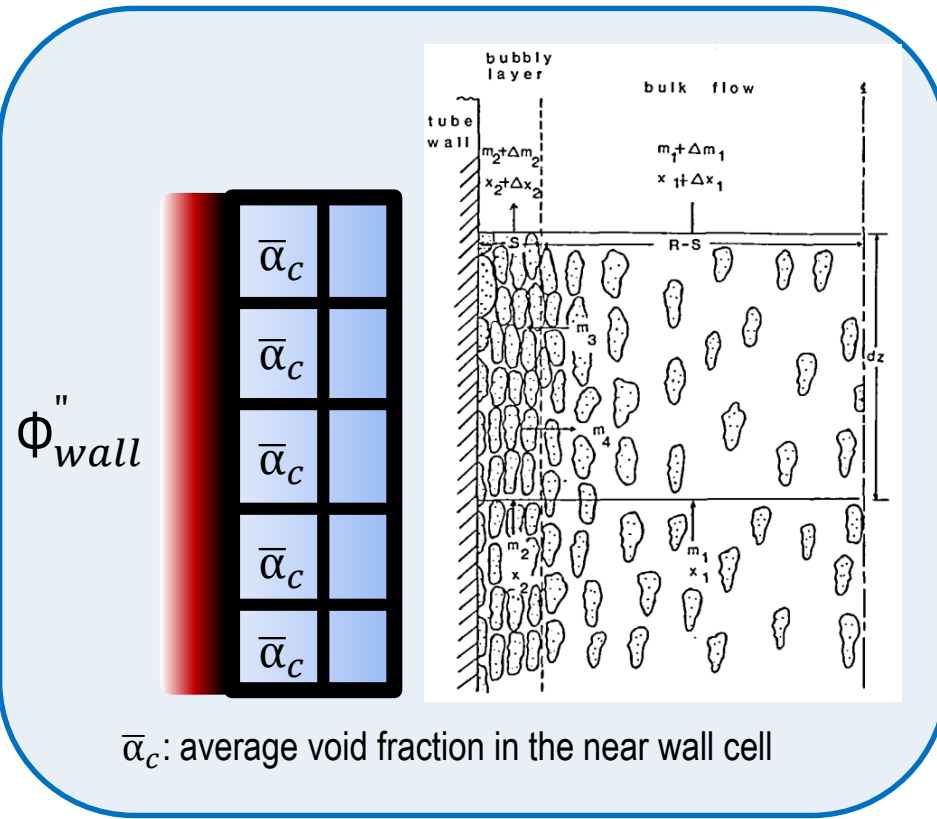
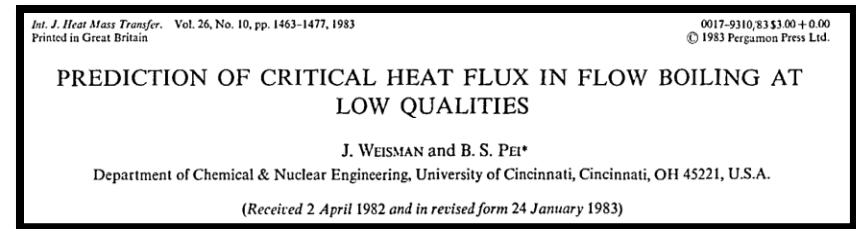
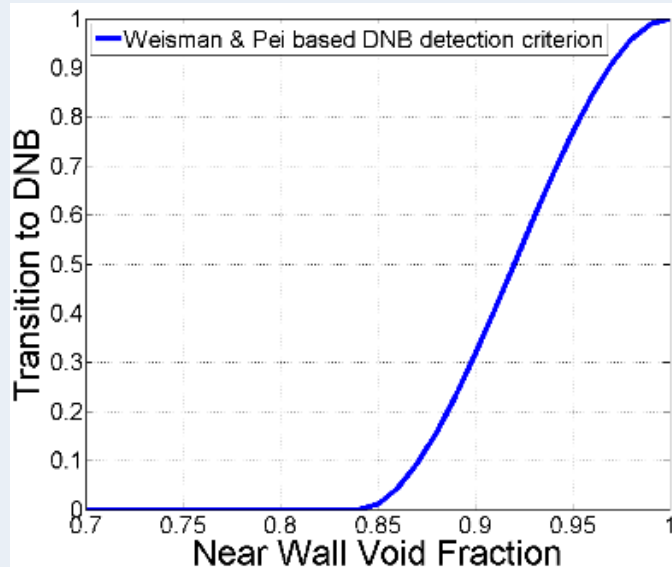


GEN-I Many variants but one approach...

• DNB Forcing Function

$$\Phi''_{wall} = (1 - f) \times (\Phi''_{fc} + \Phi''_q + \Phi''_{ev}) + f \times \Phi''_{gas}$$

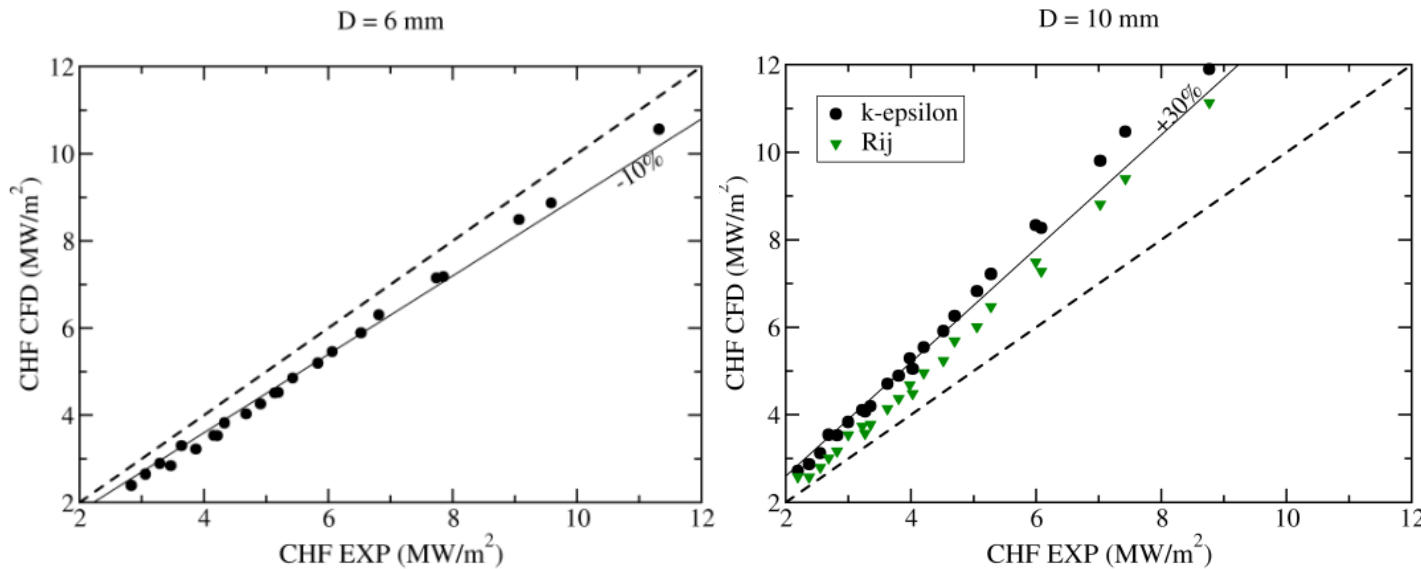
- A priori Heat Transfer mode transition
- Bubbly layer theory. Critical near-wall void fraction
- $\alpha_c = 0.82$ (Weisman & Pei 1983)
- f = smooth blending function between 0 and 1



$\bar{\alpha}_c$: average void fraction in the near wall cell

GEN-I attempts at calibration...

8



- Low errors in optimized cases
- High errors non standard cases
- High sensitivity on:
 - Mesh
 - Physics models
- Could be partly related to limitations of the Hydrodynamic closures

CFDMSRS-5, September 9-11 2014, Zurich, Switzerland

COMPUTATIONAL MULTI-FLUID DYNAMICS PREDICTIONS OF CRITICAL HEAT FLUX IN BOILING FLOW

S. Mimouni, C. Baudry, M. Guingo, J. Lavieville, N. Merigoux, N. Mechtoua

Electricité de France, R&D Division, 6 Quai Watier, 78401 Chatou, France

stephane.mimouni@edf.fr

ExHFT-7
28 June - 03 July 2008, Krakow, Poland

ANALYSIS OF TWO-PHASE FLOWS IN PIPES AND SUBCHANNELS UNDER HIGH PRESSURE

N. Alleburn¹, R. Reinders¹, S. Le², A. Splawski²

¹ AREVA, AREVA NP GmbH, Paul-Gossen Str. 100, 91052 Erlangen, Germany
² CD-adapco, G3, Trident House, Trident Park, Basil Hill Road, Didcot, OX11 7EJ, UK

ICONE21-15345

DEPARTURE FROM NUCLEATE BOILING MODELING DEVELOPMENT FOR PWR FUEL

Jin Yan, L. David Smith III, Zeses Karoutas

Westinghouse Electric Company LLC, 5801 Bluff Road, Hopkins, SC, 29061
yanj@westinghouse.com

CFD SIMULATION OF CRITICAL HEAT FLUX IN A TUBE

L. Vyskocil, J. Macek

Nuclear Research Institute Rez (NRI), Dept. of Thermal Hydraulic Analyses, 250 68 Rez, Czech Republic

Prediction of CHF in vertical heated tubes based on CFD methodology

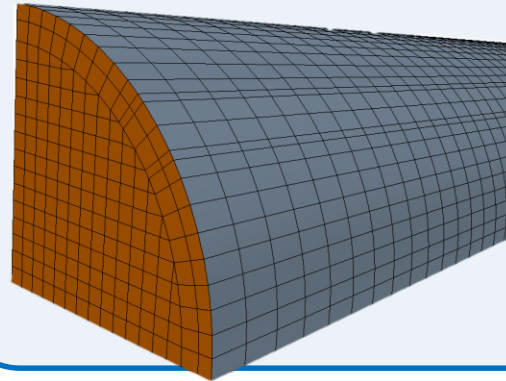
Rui Zhang, Tenglong Cong, Wenxi Tian, Suizheng Qiu, Guanghui Su¹

School of Nuclear Science and Technology, State Key Laboratory of Multiphase Flow in Power Engineering, Xi'an Jiaotong University, Xi'an 710048, China

1. Implementation of “Gen I” DNB Model

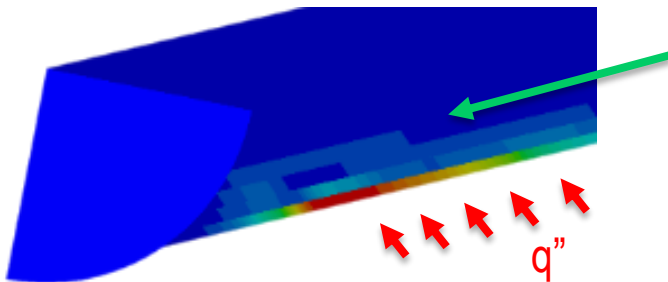
LANL in charge of assessment will present current status

Currently working on 5x5 application



- Single tube (8mm)
- Pressure: 100 bar
- Inlet quality: -0.24
- Inlet mass flux: $3000 \frac{\text{kg}}{\text{m}^2\text{s}}$
- Constant heat flux
- Reference CHF: Groeneveld 2006
- Constant lift

0.025 Lift Coefficient

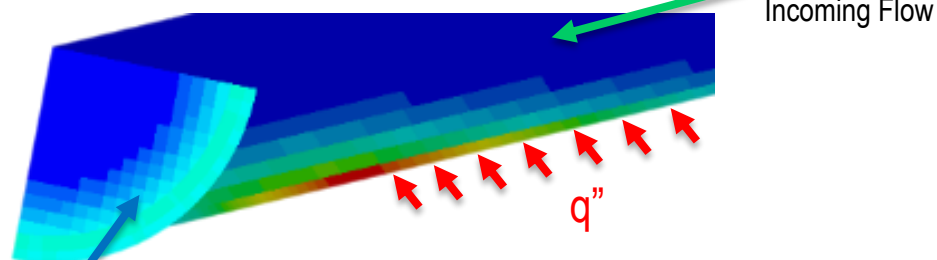


$$Q_{CFD} = 4.35\text{MW}$$

$$Q_{LUT} = 5.189\text{MW}$$

$$\varepsilon = -16.2\%$$

No Lift

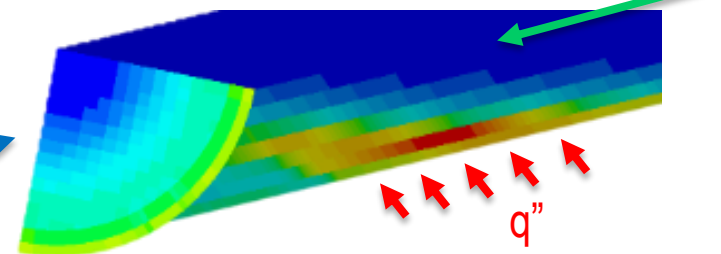


$$Q_{CFD} = 5.04\text{MW}$$

$$Q_{LUT} = 4.666\text{MW}$$

$$\varepsilon = 8\%$$

-0.025 Lift Coefficient



$$Q_{CFD} = 5.0\text{MW (no DNB)}$$

$$Q_{LUT} = \emptyset$$

$$\varepsilon > 30\%$$

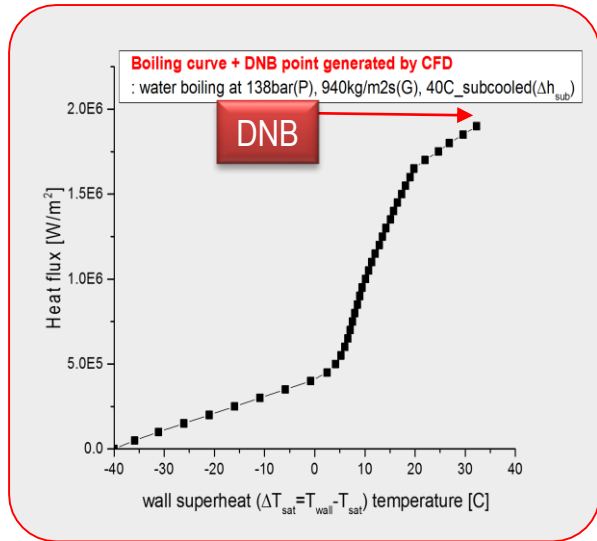
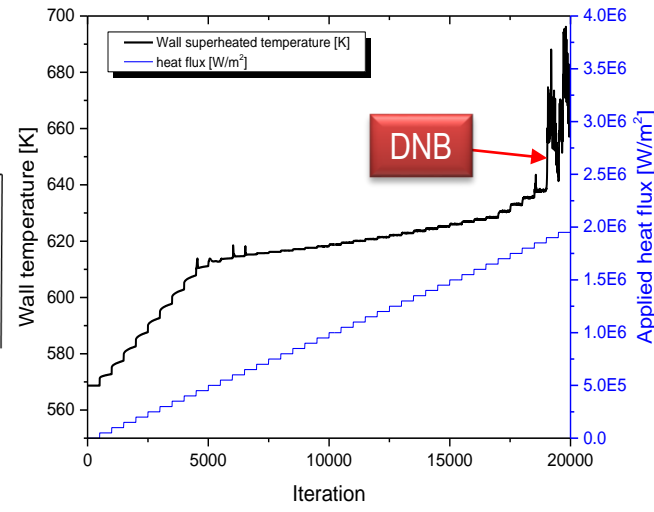
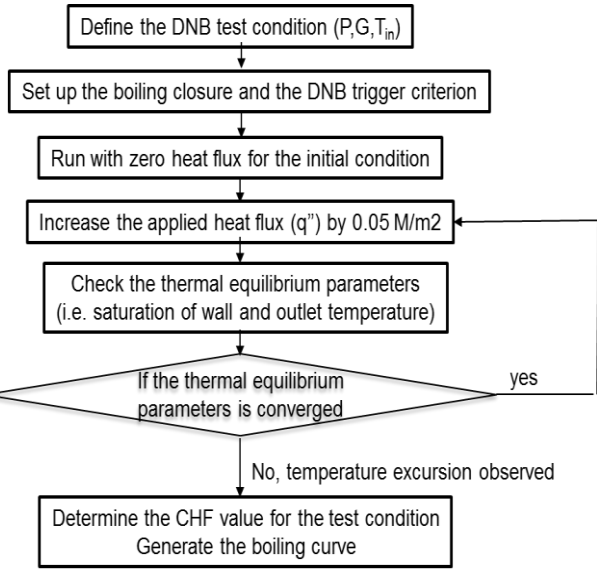
Outlet Boundary

CFD methodology for DNB model and boiling curve generation

CFD methodology for DNB model

Wall temperature monitoring

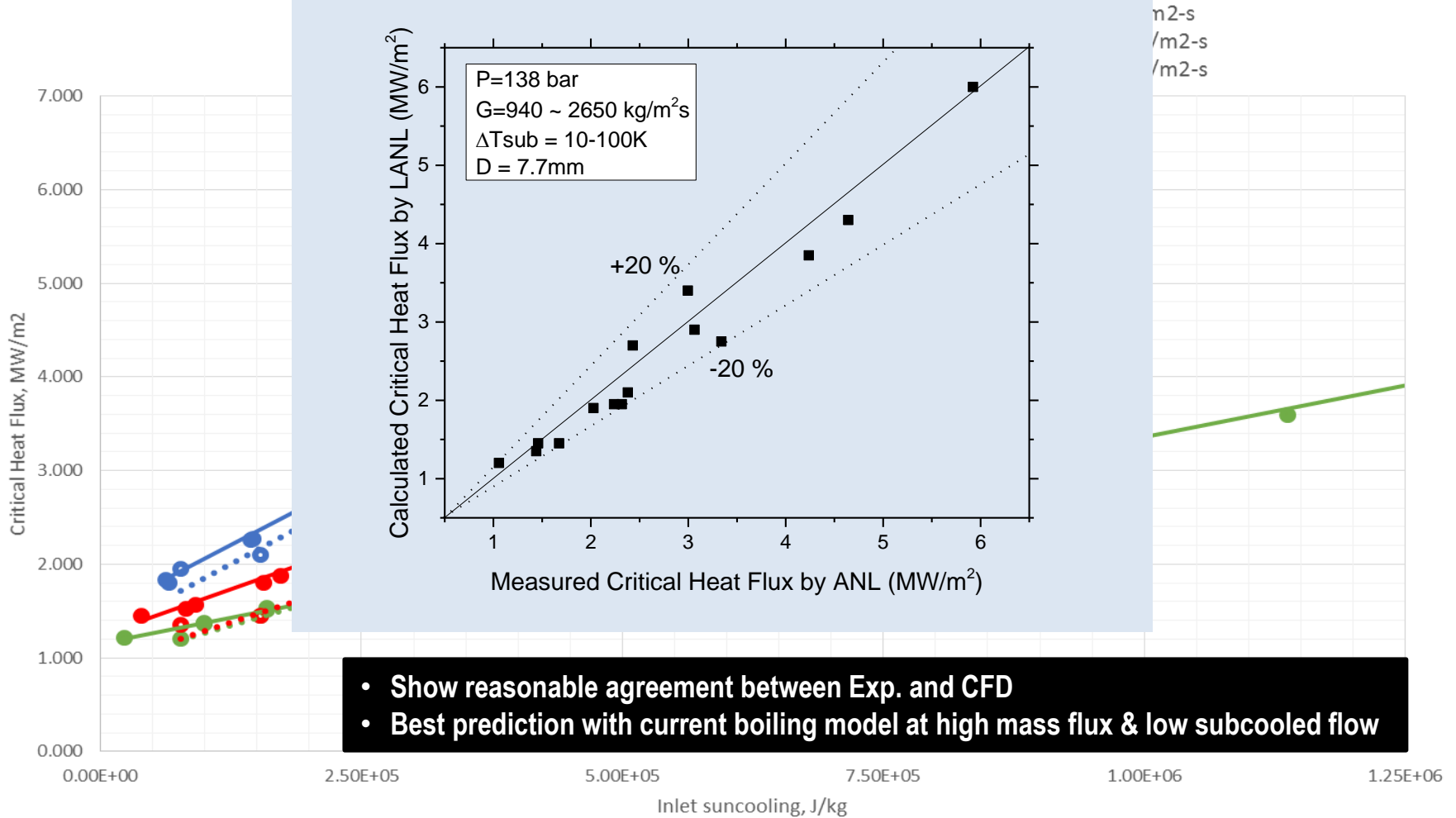
Boiling curve with DNB point



Jun Kim – LANL , Etienne Demarly - MIT

Preliminary result for DNB validation in M-CFD

The effect of Inlet Subcooling on DNB value shown in both EXP(Weatherhead, 1963) and CFD (LANL,2016)

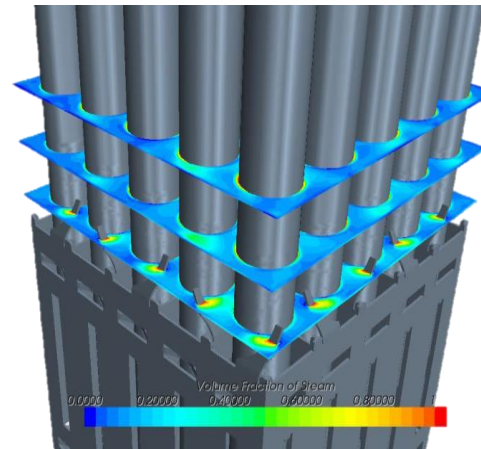
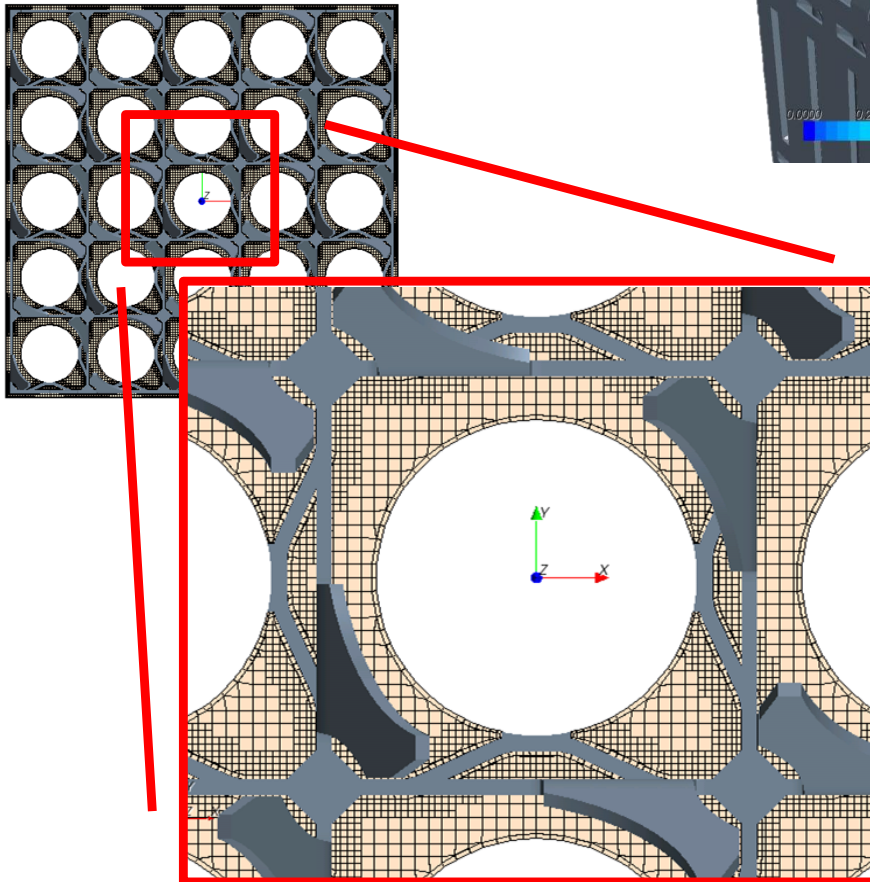


- Show reasonable agreement between Exp. and CFD
- Best prediction with current boiling model at high mass flux & low subcooled flow

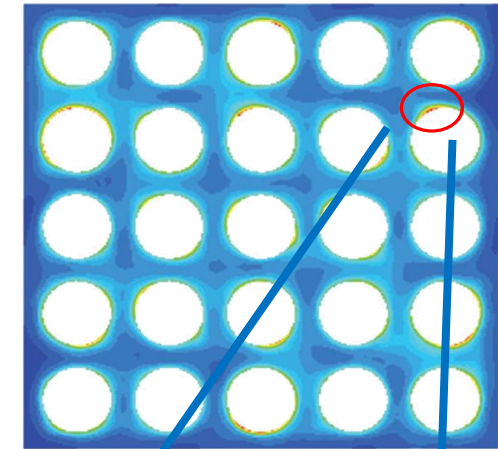
Jun Kim – LANL
Etienne Demarly - MIT

PWR Fuel Geometries

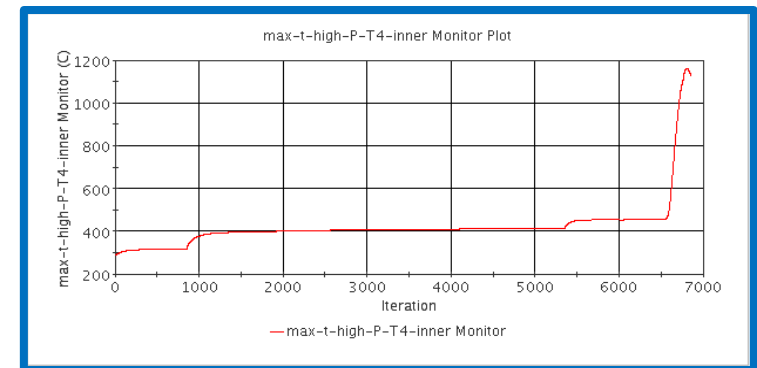
- Currently starting evaluating model applicability and BPG for 5x5 assembly



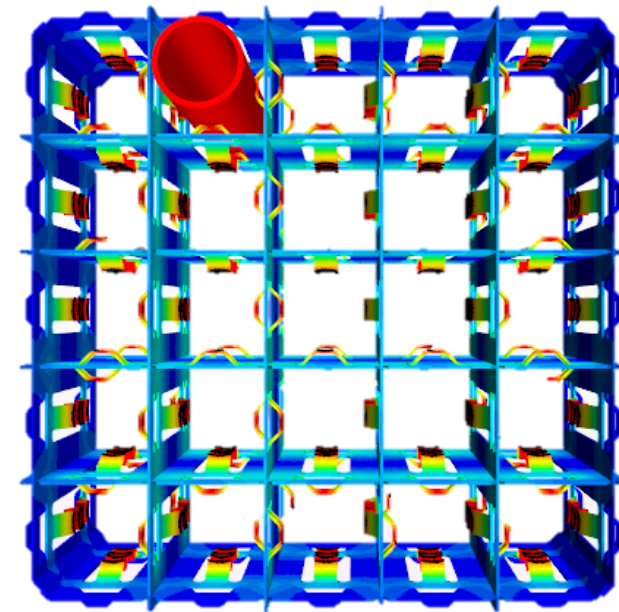
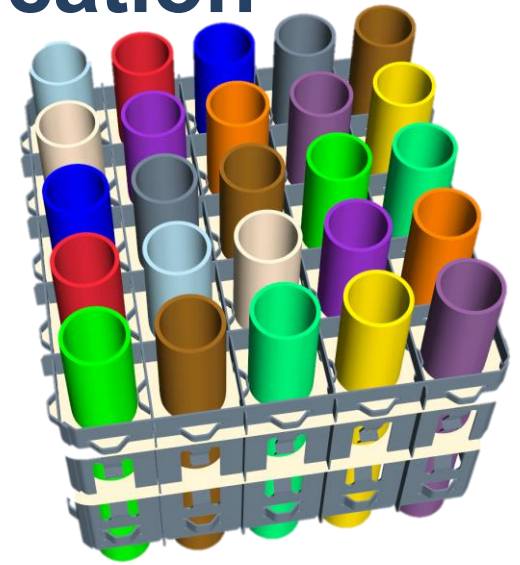
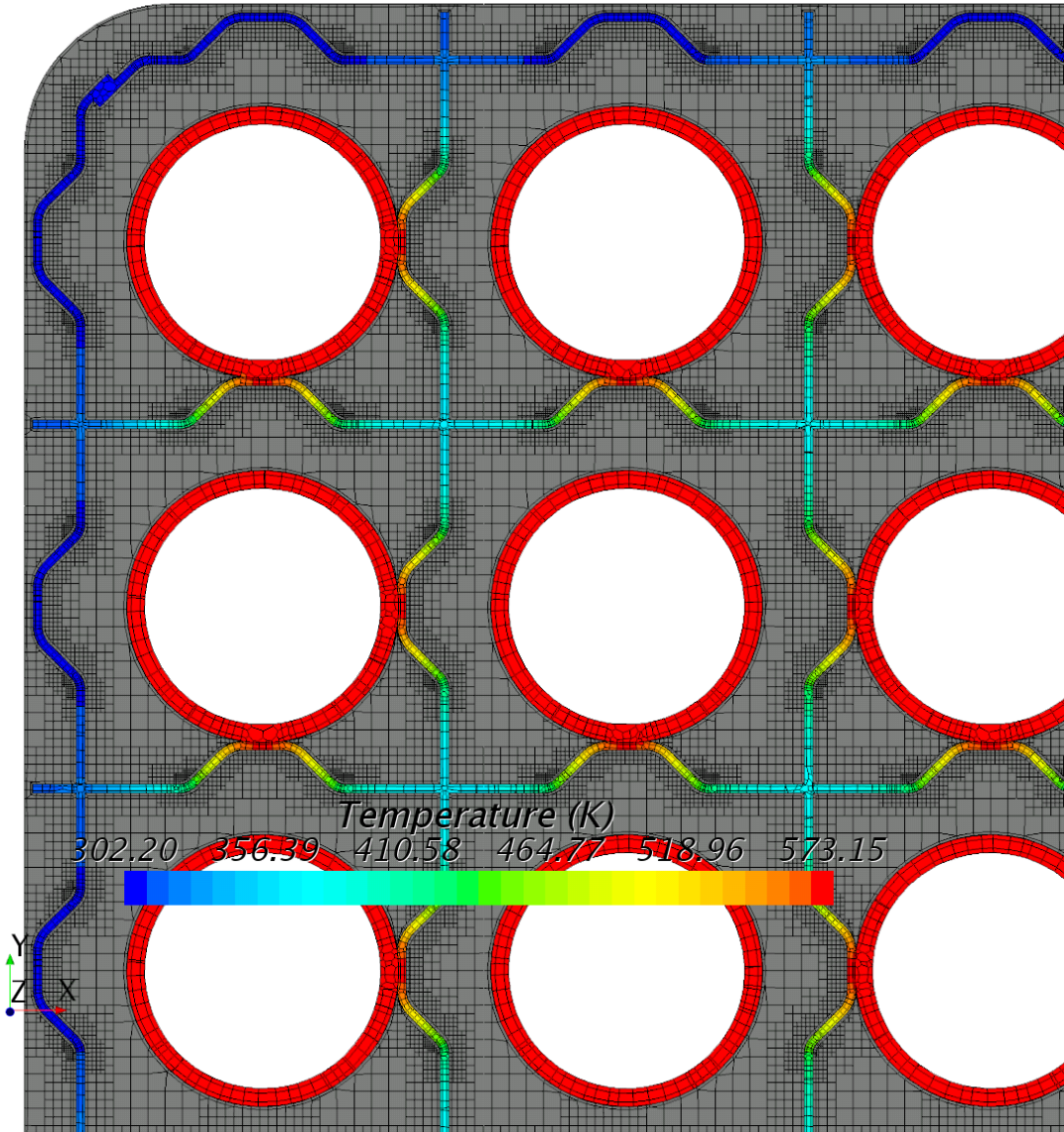
void fraction



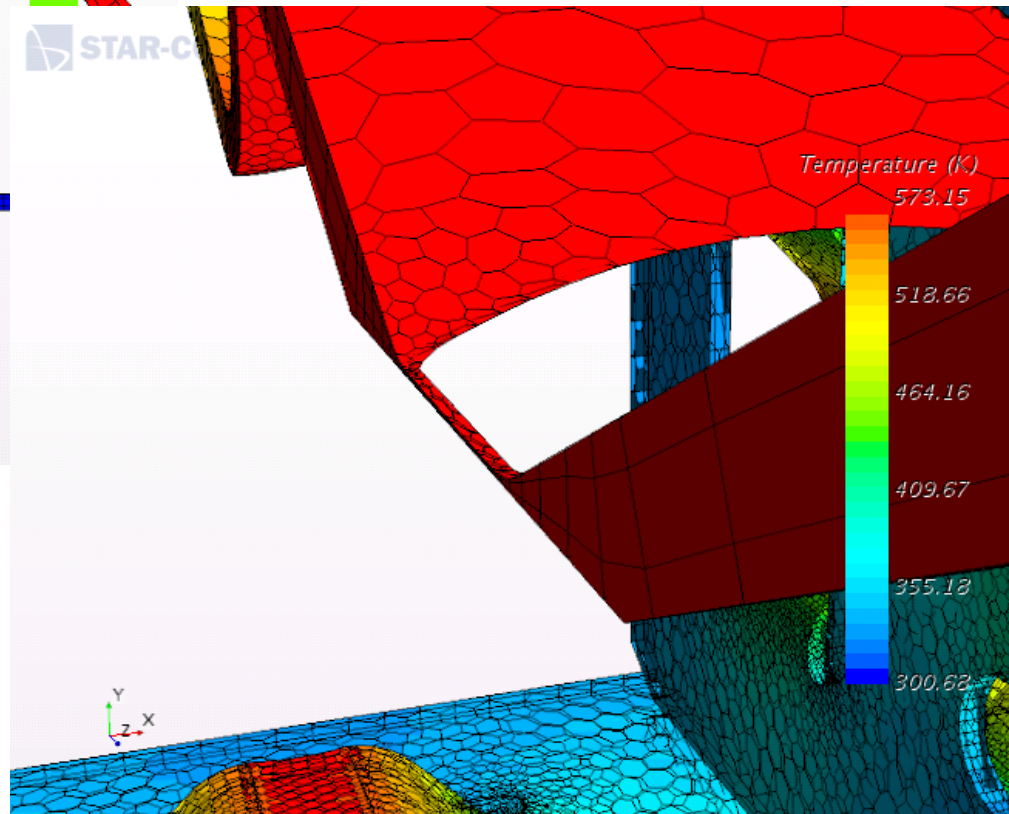
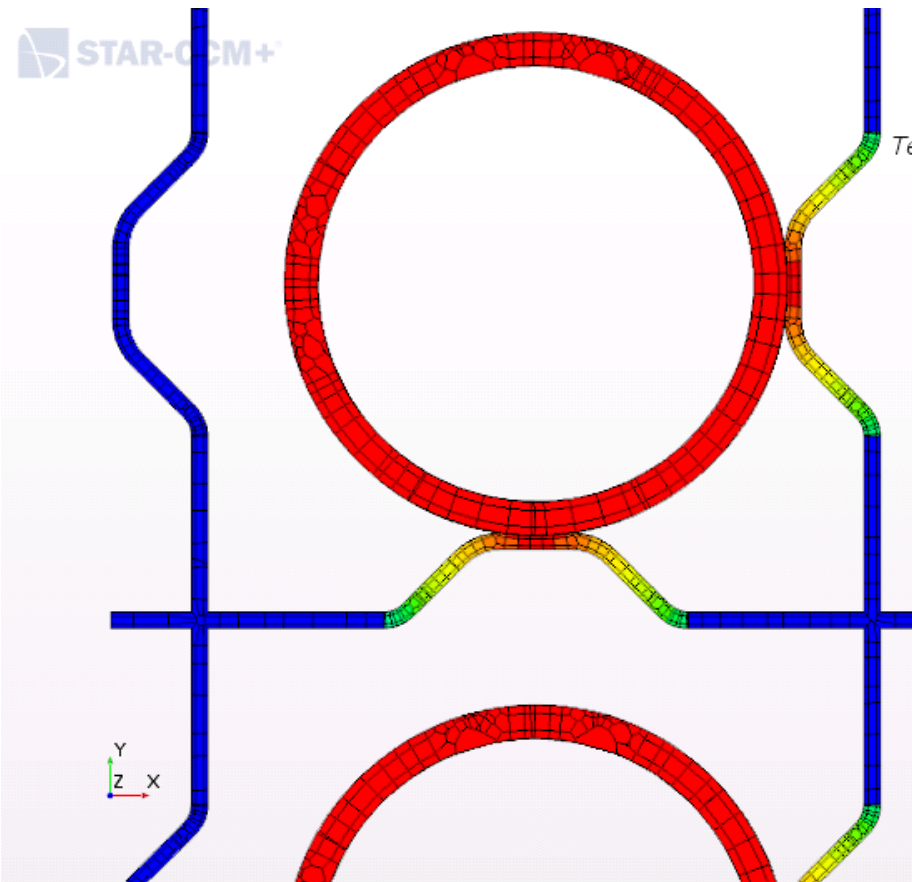
DNB



Challenges of “industrial” application

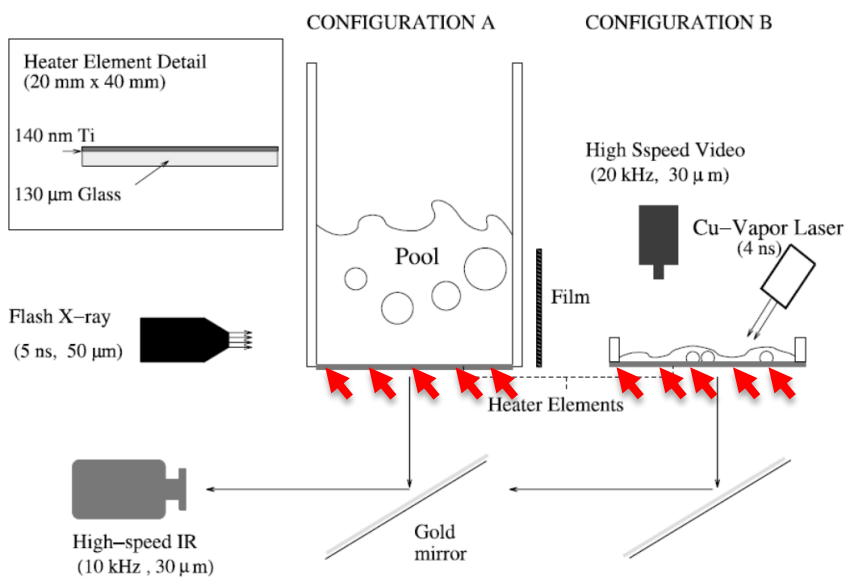


Challenges of “industrial” application



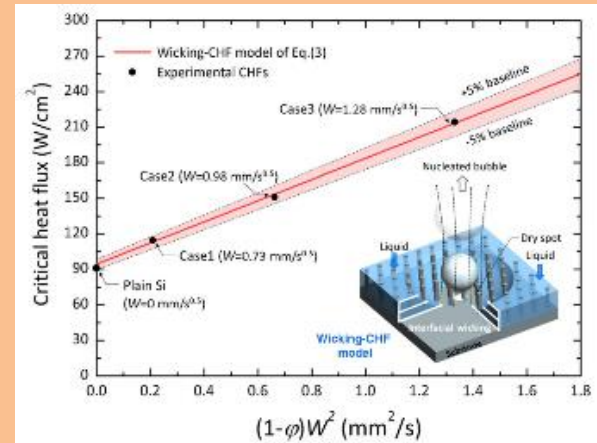
DNB Experimental Observation

Macro vs Micro thermal hydraulic origin of DNB



Y. Liu, M. Srivastava, N. Dinh... CASL Report: L3:THM.CLS.P9.06

Micro/nano surface CHF enhancements



B. Kim, H. Lee. Interfacial wicking dynamics (...) 2014

Dry Area Fraction

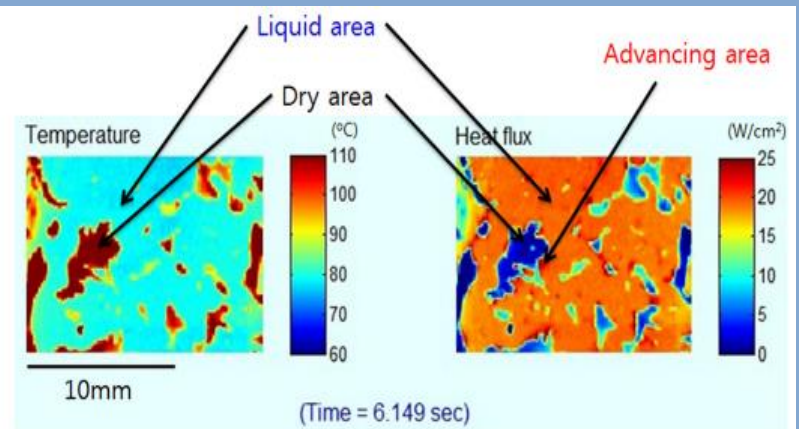


Fig. 7 Temperature and heat flux distribution at $q'' = 15.7 \text{ W/cm}^2$ for two successive frames

J. Jung, S. J. Kim. Observations of the CHF process (...) 2014

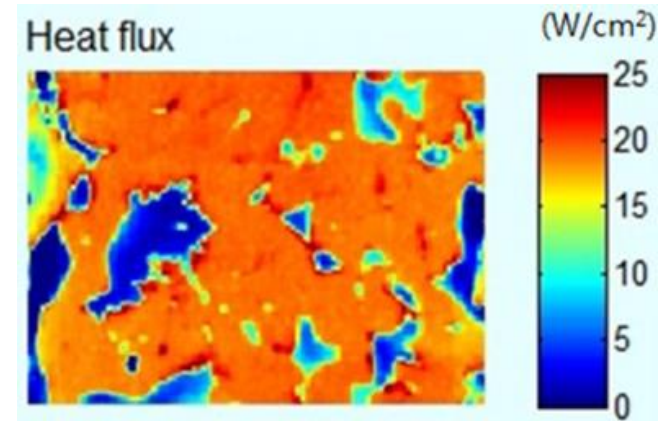
2. Develop a consistent new DNB representation in CFD based

$$\Phi''_{wall} = (1 - f) \times \Phi''_{NB} + f \times \Phi''_{gas}$$

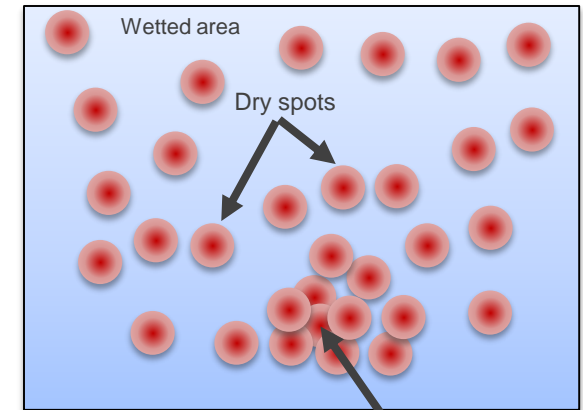
$$f = \frac{A_{Dry}}{A_{Dry} + A_{Wet}}$$

Parameters of importance for f :

$A_{Dry}(N'', t_w, t_g, D_d, \dots)$
+ Surface properties (surface tension, cavities, C_p)
+ Dry Spot clustering dynamics



Heater surface



2. Develop a consistent new DNB representation in CFD

Single-phase (liquid) forced convection

$$\Phi_{fc}'' = \frac{\rho_l c_{pl} u_\tau}{t^+} (\Delta T_{sup} + \Delta T_{sub})$$

Evaporation via bubble generation

$$\Phi_{ev}'' = \frac{4}{3} \pi \left(\frac{D_d}{2}\right)^3 \rho_g h_{fg} f N''$$

Quenching

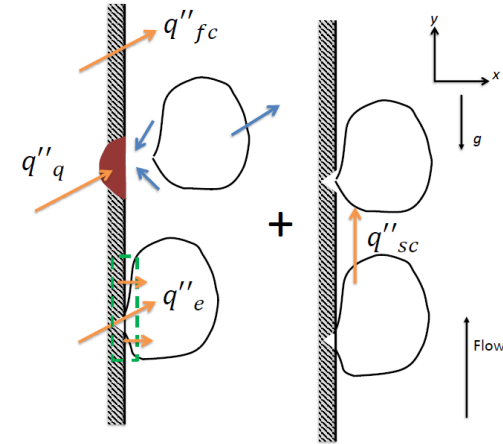
$$\Phi_q'' = \rho_h c_{ph} \Delta T_h V_q f N''$$

Sliding conduction (sliding bubbles)

$$\Phi_{sc}'' = \frac{2k_l(T_w + T_l)}{\sqrt{\pi\eta_l t^*}} a_{sl} t^* f N''^*$$

$$\Phi_{wall}'' = (1 - f) \times (\Phi_{fc}'' + \Phi_q'' + \Phi_{ev}'' + \Phi_{sc}'') + f \times \Phi_{gas}''$$

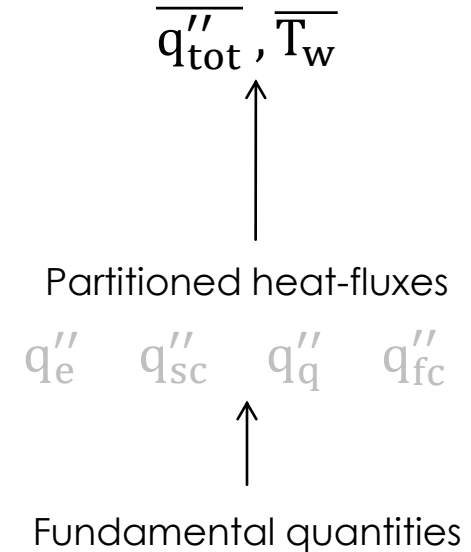
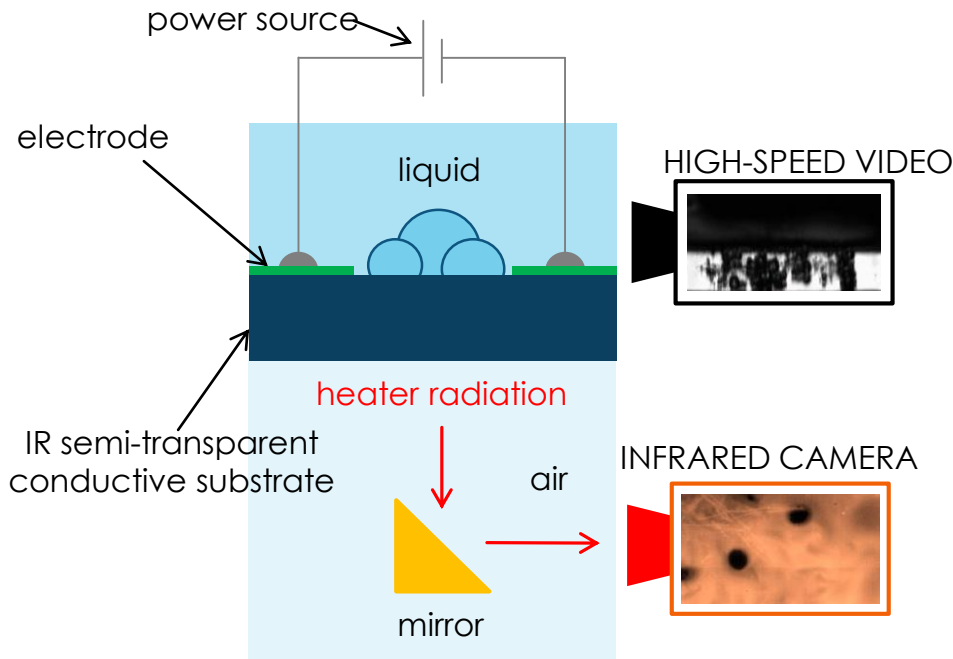
Single phase heat flux to the gas phase



Depiction of the heat flux partitioning for subcooled flow boiling.

Drive development with measurements

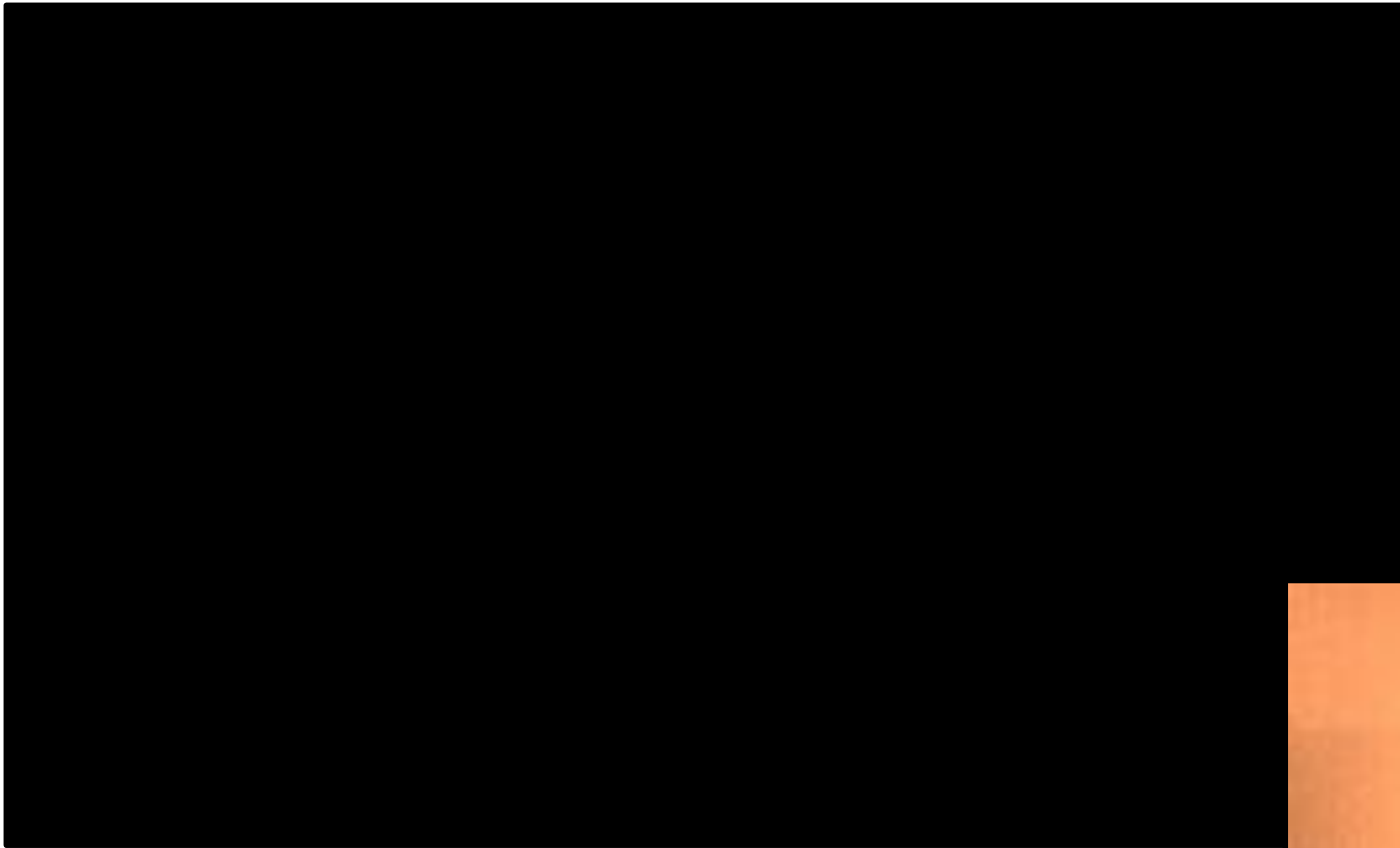
High-speed IR phase detection and high-speed video



- Average temperature and heat flux
- Nucleation site density
- Bubble departure frequency
- Bubble departure and lift-off diameter
- Sliding distance

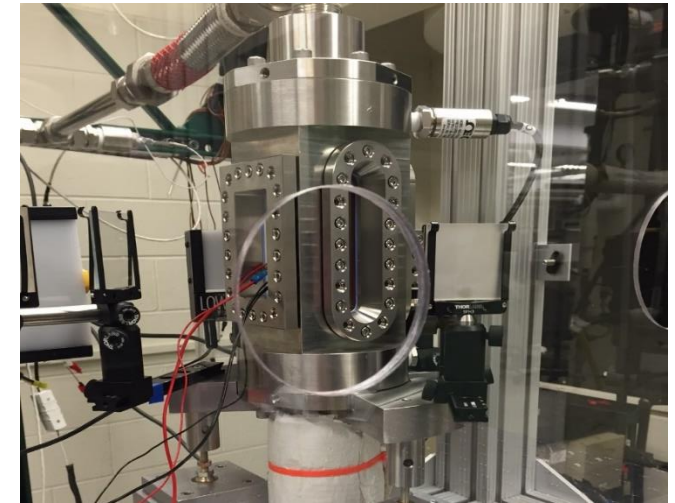
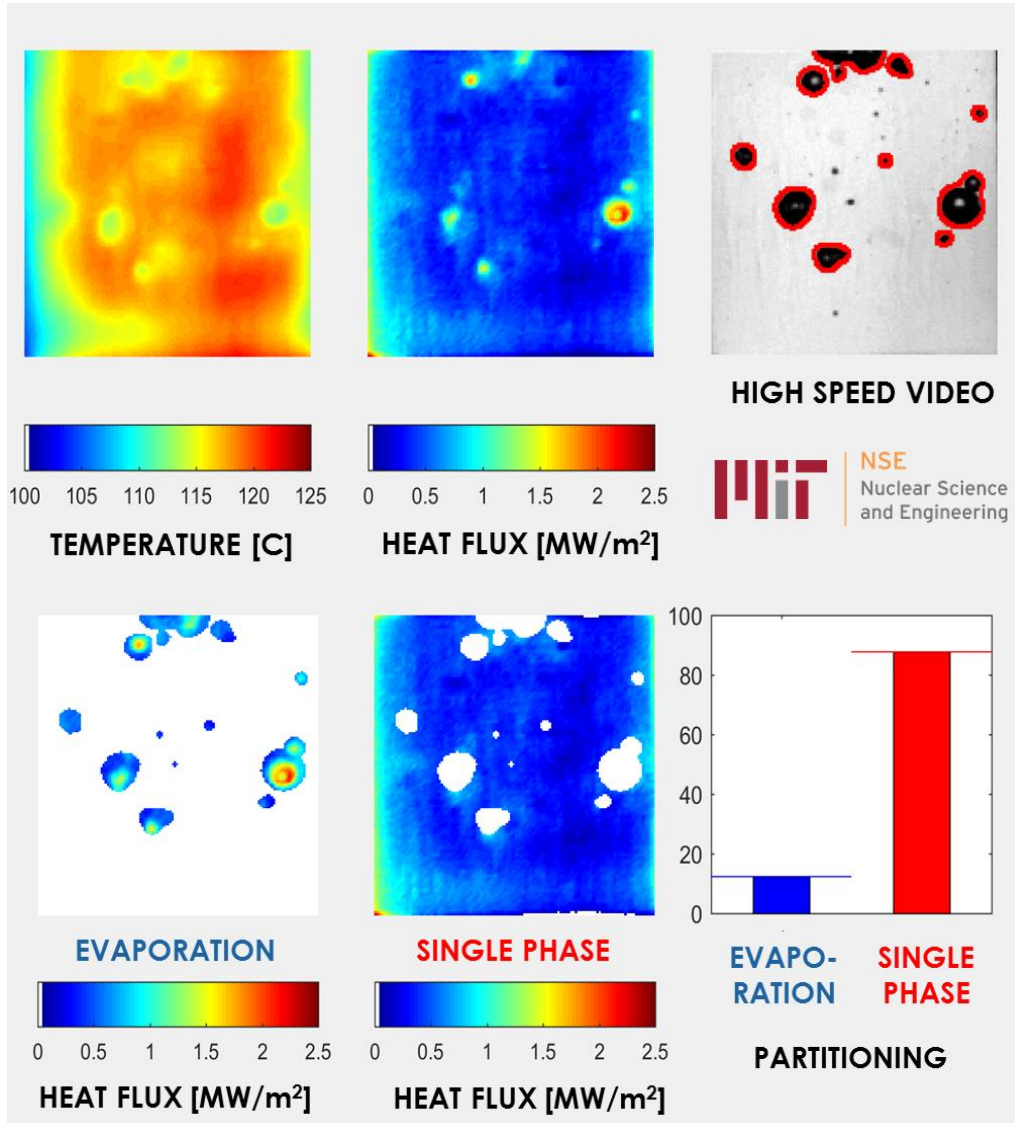
$$N_d \quad t_w \quad t_g \quad f \quad D_d \quad D_l \quad h_{fc} \quad d_{sl} \quad A_{wet} \quad l_{cl} \dots$$

Examples of IR phase detection capabilities



zoom on a nucleation site

3. GEN-II Experiment for High Heat Flux



PEThER

- Up to 10 bars
- Ambient temperature to saturation
- 400 to 1250 kg/m²/s
- Up to CHF
- Synchronized IR and HSV
- **Advanced post-processing algorithms**

ENABLE DIRECT MEASUREMENT OF HEAT FLUX PARTITIONING

Driven by *new data analysis techniques*

Nucleation Sites interaction

The current best practice for NSD modeling is the Hibiki-Ishii correlation (2003).

- Semi-empirical modeling of cavity activations on the heater
- Correlation behavior is exponential by nature and **unbounded**.
- Impossible to use as-is in a numerical simulation
- In reality, there are only so many bubbles a surface can sustain.

$$N_{HI}''(\Delta T) \propto e^{k\Delta T}$$

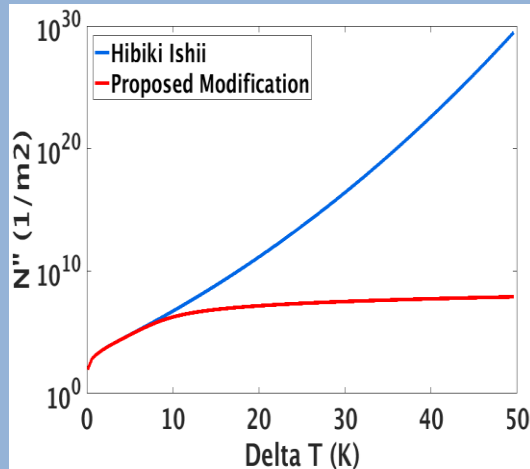
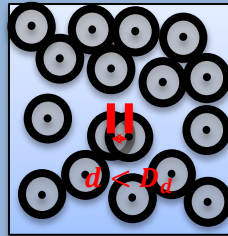
Number of activated cavities \neq Number of active bubble generating sites.

Complete Spatial Randomness:

$$P = 1 - e^{(-\pi D_d^2 N'')}$$

Proposed modification to Hibiki-Ishii correlation:

$$N_{mod}''(\Delta T) = N_{HI}''(\Delta T) e^{-\pi D_d^2 N_{mod}''(\Delta T)}$$

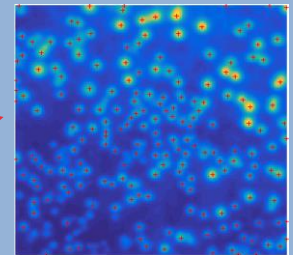


Automatic data post-processing framework

Nucleation site Detection via IR post-processing

1. Creation of a metric:

$$F(x, y) = \max_{k=0}^{N_{max}} \left| \frac{T(x, y, k+1) - T(x, y, t)}{\Delta t} \right|$$



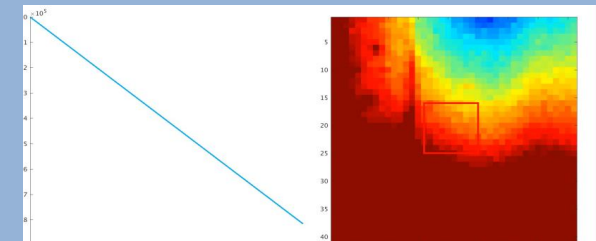
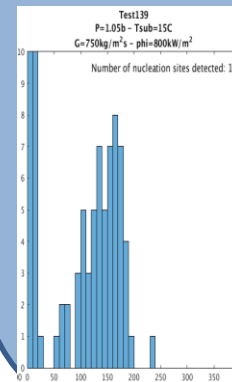
2. Gaussian smoothing (optional)

3. Detection of local maxima

4. Binary masking

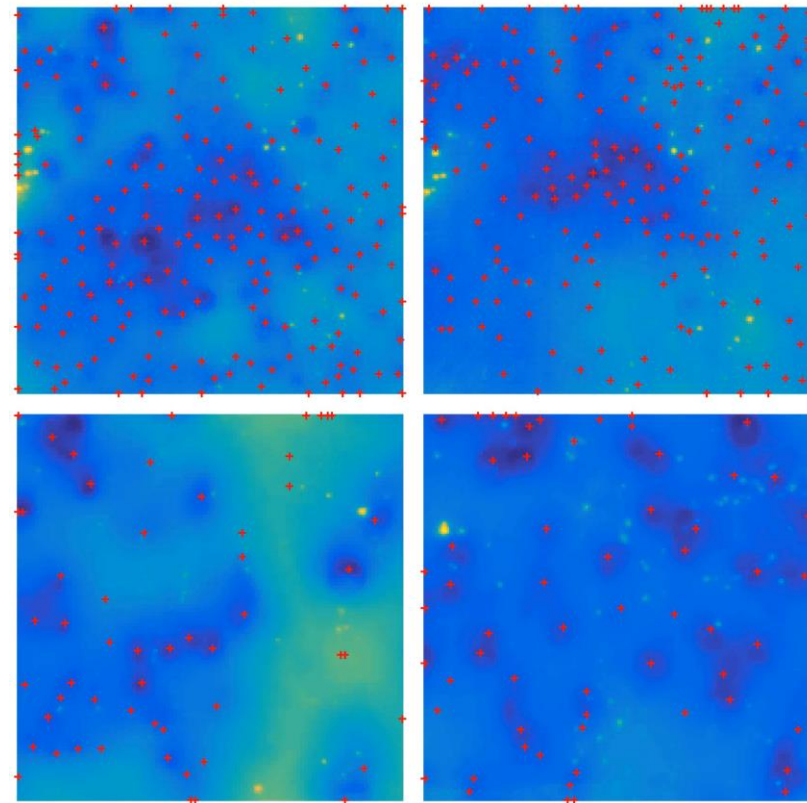
5. Individual site frequency analysis

6. Spectral analysis of the departure frequency for each case



MIT Flow Boiling experiment (2013)

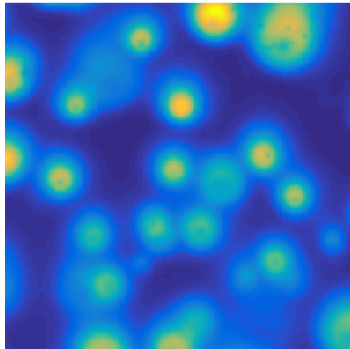
- High speed IR camera acquisition
- Post-processing of T and ϕ''
 - Nucleation site detection
 - Frequency analysis



Time integral of the Temperature/Heat Flux derivative (rate of change) + pre/post processing

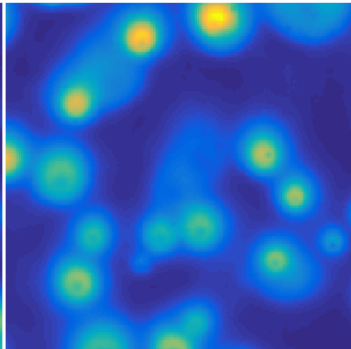
Test293

$P=1.5b - G=150kg/m^2s$
 $T_{sub}=10C - \phi=600kW/m^2$



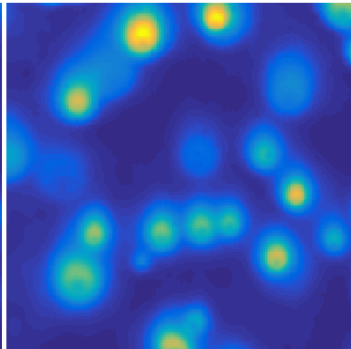
Test303

$P=1.5b - G=250kg/m^2s$
 $T_{sub}=10C - \phi=600kW/m^2$



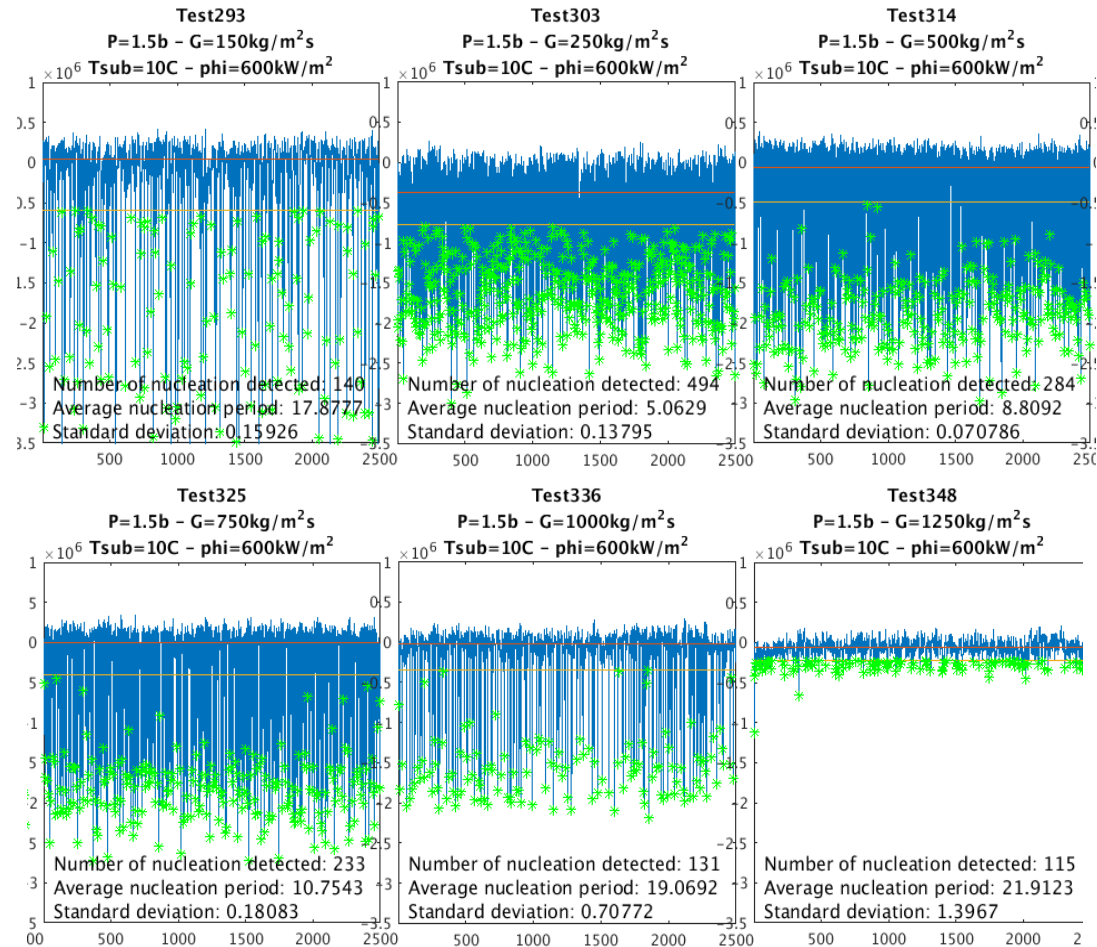
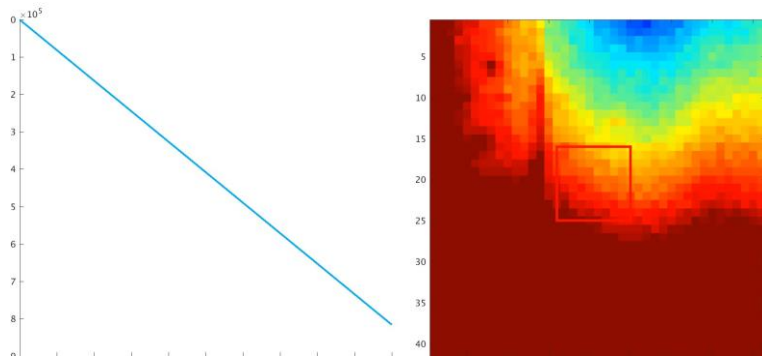
Test314

$P=1.5b - G=500kg/m^2s$
 $T_{sub}=10C - \phi=600kW/m^2$



Frequency Analysis

- From a nucleation site location:
 - Signal extraction
 - Detection of nucleation events
 - Statistical analysis (mean, std)
 - Dependency to TH conditions for the same site
 - Statistical distribution for each case



FY17 Milestones

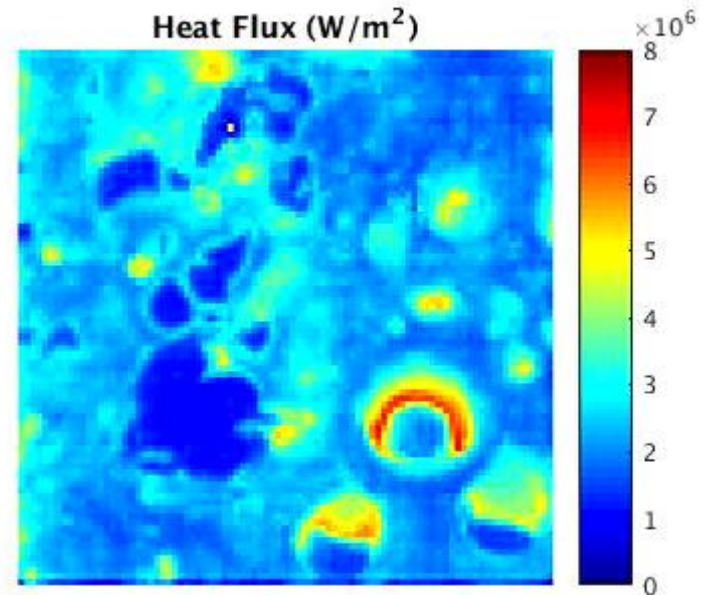
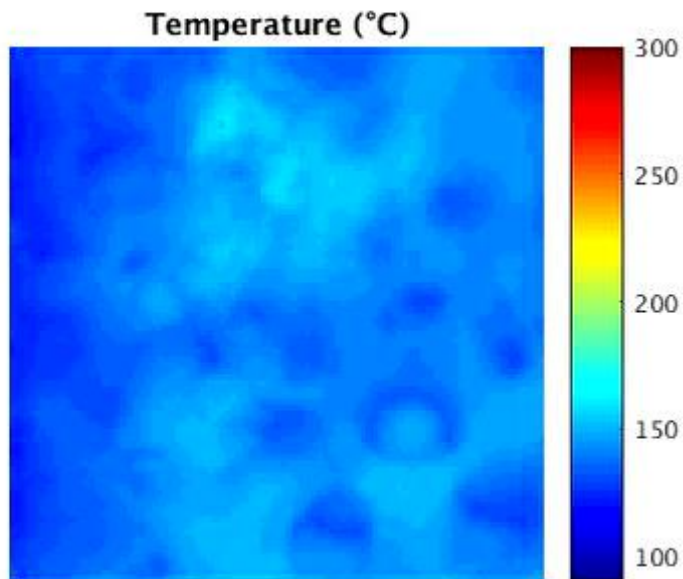
#1948	L1:CASL.P15.01	new	Baglietto	PoR-15
Develop, Demonstrate and Assess Advanced CFD-based Capability for Prediction of DNB				
#1660	L2:THM.P15.01	new	R. Brewster	PoR-15
1-Industrial DNB Method Assessment				
#1661	L2:THM.P15.02	new	Baglietto	PoR-15
GEN-II DNB Method Completion and Assessment				
#1718	L3:THM.CLS.P15.13	new	Buongiorno	PoR-15
Full Scope DNB Tests with dedicated post processing				
#1699	L3:THM.CFD.P15.06	new	Pointer	PoR-15
STAR-CCM+ V&V Assessment Report for DNB				
#1705	L3:THM.CLS.P15.02	new	Seung Jun Kim	PoR-15
GEN-II DNB Testing and Validation				
#1706	L3:THM.CLS.P15.03	new	Dinh	PoR-15
Data Driven DNB advancements				
#1708	L3:THM.CLS.P15.05	new	Baglietto	PoR-15
Hydrodynamic Closures for DNB				

CHF flow boiling experiments at MIT

IR space resolution 100 μm

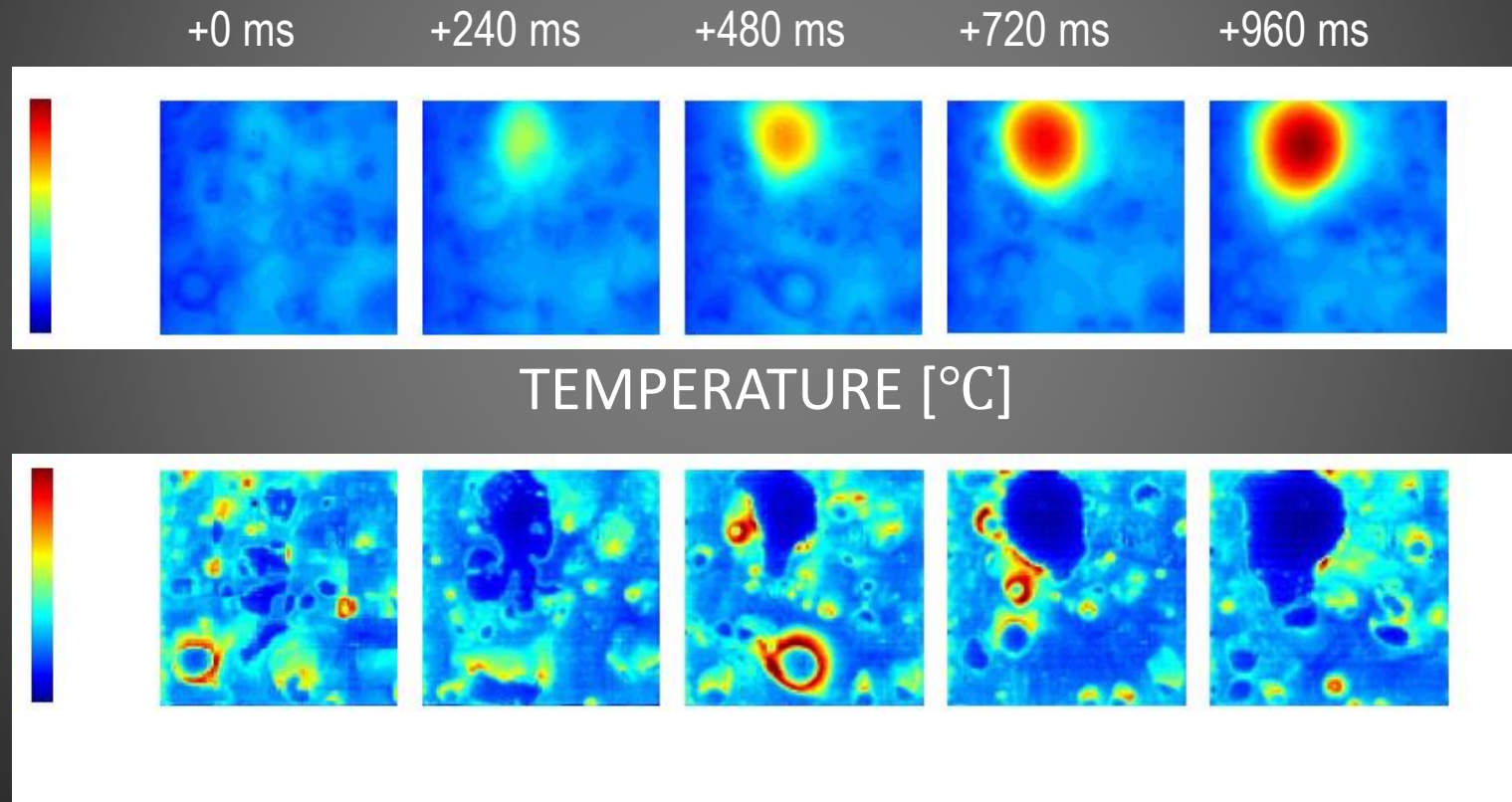
IR time resolution 0.4 ms

10K SUBCOOLED 1BAR 500 $\text{kg/m}^2\text{s}$ 2450 W/m^2 0.0 ms



Growth of the dry spot at 2.45 MW/m²/K

10 K subcooling, 500 kg/m²/s, 1 atm





www.casl.gov